Elementary Steps in the Acquisition of Mn^{2+} by the Fosfomycin Resistance Protein (FosA)†

Bryan A. Bernat and Richard N. Armstrong*

Departments of Biochemistry and Chemistry and the Center in Molecular Toxicology, Vanderbilt University School of Medicine, Nashville, Tennessee 37232-0146

Received July 17, 2001; Revised Manuscript Received August 30, 2001

ABSTRACT: The fosfomycin resistance protein, FosA, catalyzes the Mn^{2+}-dependent addition of glutathione to the antibiotic fosfomycin, (*1R,2S*)-epoxypropylphosphonic acid, rendering the antibiotic inactive. The enzyme is a homodimer of 16 kDa subunits, each of which contains a single mononuclear metal site. Stopped-flow absorbance/fluorescence spectrometry provides evidence suggesting a complex kinetic mechanism for the acquisition of Mn^{2+} by apoFosA. The binding of $Mn(H_2O)_6^{2+}$ to apoFosA alters the UV absorption and intrinsic fluorescence characteristics of the protein sufficiently to provide sensitive spectroscopic probes of metal binding. The acquisition of metal is shown to be a multistep process involving rapid preequilibrium formation of an initial complex with release of approximately two protons ($k_{obsd} \geq 800\ s^{-1}$). The initial complex either rapidly dissociates or forms an intermediate coordination complex ($k > 300\ s^{-1}$) with rapid isomerization ($k \geq 20\ s^{-1}$) to a set of tight protein−metal complexes. The observed bimolecular rate constant for formation of the intermediate coordination complex is $3 \times 10^5\ M^{-1}\ s^{-1}$. The release of Mn^{2+} from the protein is slow ($k \approx 10^{-2}\ s^{-1}$). The kinetic results suggest a more complex chelate effect than is typically observed for metal binding to simple multidentate ligands. Although the addition of the substrate, fosfomycin, has no appreciable effect on the association kinetics of enzyme and metal, it significantly decreases the dissociation rate, suggesting that the substrate interacts directly with the metal center.

The fosfomycin resistance protein, FosA, is a member of a functionally diverse metalloenzyme (vicinal oxygen chelate or VOC[1]) superfamily that includes glyoxalase I, the extradiol dioxygenases, and methylmalonyl-CoA epimerase (*1*−*6*). The enzyme catalyzes the Mn^{2+}-dependent addition of glutathione to the antibiotic fosfomycin, (*1R,2S*)-epoxypropylphosphonic acid, rendering it inactive (*1, 7*). The protein is a homodimer of 16 kDa subunits, each of which harbors a single mononuclear metal site. The VOC superfamily members have cup-shaped metal binding sites composed of paired $\beta\alpha\beta\beta\beta$ motifs (*8, 9*). The motifs are arranged in a pseudo-two-fold symmetric fashion so as to supply three or four protein ligands for metal binding. Sequence alignments and the metal binding characteristics and catalytic properties of site-directed mutants indicate that the Mn^{2+} binding site of FosA is composed of three ligands supplied by the protein, H7, H67, and E113 (*4*). The octahedral coordination sphere in the $E{\cdot}Mn^{2+}$ complex is completed by three water molecules (*1*). One or more of the water ligands are thought to be displaced upon binding the substrate fosfomycin. The fully activated enzyme−substrate complex also contains the monovalent cation, K^+ (*4*).

Metal-free FosA (apoFosA) is quite stable, although essentially catalytically inactive, in the absence of divalent cations. Both FosA and apoFosA are homodimeric species. In the absence of substrate the metal center is composed entirely of ligands supplied by protein side chains and solvent molecules and involves no other chelate species or cofactors. All of these factors suggest that FosA is a tractable system for examining the mechanism of metal binding. Although dozens of metalloproteins have been characterized with respect to their structure and thermodynamic stability, comparatively few mechanistic studies of the elementary steps involved in the acquisition of metals by proteins have appeared. The kinetics of binding and dissociation of metals from proteins are influenced by a number of factors including solvent/ligand dissociation rates (*10, 11*), multistep organization of the ligand set about the metal (*12*−*15*), and even the hydrophobic environment of the binding site (*16*).

In this paper we provide evidence for a multistep kinetic mechanism for the binding of $Mn(H_2O)_6^{2+}$ by apoFosA. The acquisition of metal involves rapid preequilibrium formation of an initial complex with the release of between one and two protons. The initial complex forms a spectroscopically detectable intermediate coordination complex that leads to a set of tight coordination complexes. The addition of the substrate, fosfomycin, has little effect on the association kinetics of enzyme and metal but does decrease the dissociation rate.

EXPERIMENTAL PROCEDURES

Materials. Fosfomycin disodium salt and 4-(2-hydroxyethyl)piperazine-1-ethanesulfonic acid (HEPES) were purchased from Fluka (Ronkonkoma, NY). Glutathione was

† Supported by National Institutes of Health Grants R01 AI42756, P30 ES00267, and T32 ES07028.

* Author to whom correspondence should be addressed [telephone (615) 343-2920; fax (615) 343-2921; e-mail r.armstrong@vanderbilt.edu].

[1] Abbreviations: GSH, glutathione; HEPES, 4-(2-hydroxyethyl)-piperazine-1-ethanesulfonic acid; EDTA, ethylenediaminetetraacetic acid; TMA, tetramethylammonium; VOC, vicinal oxygen chelate.

10.1021/bi0114832 CCC: $20.00
Published on Web 09/29/2001

obtained from Sigma (St. Louis, MO). Tetramethylammonium (TMA) chloride and TMA hydroxide were purchased from Aldrich (Milwaukee, WI). KCl and NH_4Cl were purchased from Mallinckrodt (Paris, KY). $MnCl_2$ was of Puratronic grade purchased from Alfa Inorganics (Ward Hill, MA). ApoFosA was prepared as previously described (*1*).

UV−Visible Spectroscopy. Spectra were acquired on a PC-controlled Perkin-Elmer Lambda 18 dual-beam, double-grating spectrophotometer at 25 °C. Scans from 240 to 340 nm were taken of 20 μM enzyme, 100 mM HEPES/KOH (pH 8.0) ± 200 μM $MnCl_2$.

Stopped-Flow Data Acquisition and Analysis. The binding of divalent cations to FosA was determined on an Applied Photophysics Ltd. model SX17MV stopped-flow spectrometer operated in the absorption or fluorescence mode at 25 °C. In the absorption mode, the wavelength was set at 245 or 297 nm using two monochromators and a path length of 1 cm. Absorbance changes at 297 nm were observed through a 15 nm narrow band-pass filter at 290 nm to eliminate unwanted fluorescence emission. For the fluorescence mode, the excitation was set at 290 nm using a double monochromator. The intrinsic protein fluorescence was observed using a 0.2 cm path length cell through a 320 nm cutoff filter. Enzyme was diluted in HEPES buffer (pH 8.0) with KOH or TMA hydroxide. Metal solutions were prepared in water. All reactions contained 5 μM enzyme, 100 mM HEPES (pH 8.0), and 60 mM KOH or TMA hydroxide unless noted otherwise. Unless otherwise noted, the reported concentrations of reagents are those in the observation cell. Each kinetic trace was the average of four to six individual experiments. When data were collected for more than 1 s, the oversampling function was used to improve the signal-to-noise ratio.

The kinetic data were fit to a single-, double-, or triple-exponential equation (eqs 1−3) when appropriate. For short

$$Y = A_0\, e^{-kt} + c \tag{1}$$

$$Y = A_{01}\, e^{-k_1 t} + A_{02}\, e^{-k_2 t} + c \tag{2}$$

$$Y = A_{01}\, e^{-k_1 t} + A_{02}\, e^{-k_2 t} + A_{03}\, e^{-k_3 t} + c \tag{3}$$

acquisition times, the first 0.002 s was ignored for fitting. For data where k_{obsd} changed as a function of the concentration of metal, the data were fit to eq 4 to determine the apparent rate constants for k_{on} and k_{off}.

$$k_{obsd} = k_{on}[\text{metal}] + k_{off} \tag{4}$$

Time-Dependent Difference Spectra. To obtain time-dependent difference spectra, data were collected in the stopped flow between 315 and 239 nm at 4 nm intervals and transferred into the Pro-Kineticist global analysis/simulation software (Applied Photophysics). The enzyme concentration was 15 μM, and the $MnCl_2$ concentration was 200 μM.

Sequential Mixing. The sequential mixing experiments were carried out on the same stopped-flow instrument reconfigured accordingly. The aging loop contained 4 μM FosA, 40 μM $MnCl_2$, 100 mM HEPES/KOH (pH 8.0), which was mixed 1:1 with 50 mM EDTA, and 100 mM HEPES/KOH (pH 8.0) after different delay times.

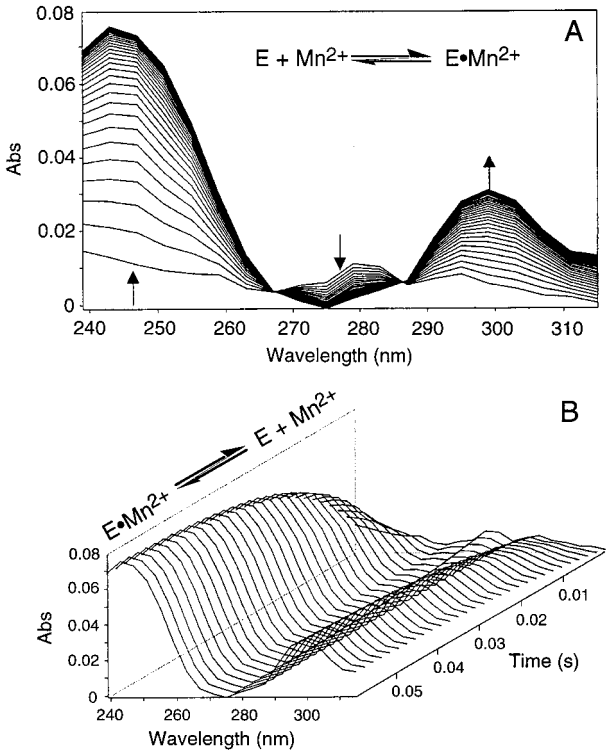

FIGURE 1: Evolution of the UV difference spectra upon rapid addition of 200 μM $Mn(H_2O)_6^{2+}$ to 15 μM FosA. Kinetic traces were acquired at 4 nm intervals between 315 and 239 nm and processed with the Pro-Kineticist program. (A) Overlay of spectra acquired at 2 ms internals for 60 ms. Arrows indicate the direction of the absorbance changes from $t = 0$. (B) Plot of the same data in three dimensions. The evolution of the difference spectra was fit to a simple approach to equilibrium with $k_{on}(\text{app}) = (2.5 \pm 0.1) \times 10^5$ M^{-1} s^{-1} and $k_{off}(\text{app}) = 13 \pm 2$ s^{-1}.

Proton Release Experiments. For experiments with the pH indicator phenol red, FosA was dialyzed exhaustively against water at 4 °C to remove buffer. Unbuffered enzyme and metal solutions containing 10 μM phenol red were adjusted to 8.0 with KOH after the solutions had been sparged with N_2. The sparging attachment on the stopped-flow instrument was used to blanket the solutions with N_2 to minimize the exposure to air and absorption of CO_2. Proton release was observed by following the change in A_{558} in the stopped flow or by titration at the same wavelength in a Perkin-Elmer Lambda 18 spectrometer.

RESULTS

Spectral Changes on Metal Binding to FosA. The binding of $Mn(H_2O)_6^{2+}$ and other divalent cations to FosA results in substantial changes in the UV spectrum and intrinsic fluorescence properties of the protein. Addition of saturating concentrations of $Mn(H_2O)_6^{2+}$ to FosA results in increases in absorbance at 245 nm ($\Delta\epsilon = 5000$ M^{-1} cm^{-1}) and 297 nm ($\Delta\epsilon = 2000$ M^{-1} cm^{-1}) and a small decrease in absorbance at 279 nm ($\Delta\epsilon = -1000$ M^{-1} cm^{-1}). In addition, the intrinsic fluorescence emission of the protein ($\lambda_{ex} = 290$ nm) is quenched by ~25%, although the maximum emission wavelength ($\lambda_{em} = 328$ nm) does not change on formation of the $E{\cdot}Mn^{2+}$ complex.

The time-dependent evolution of the UV difference spectrum of the protein at a single concentration of $Mn(H_2O)_6^{2+}$ is illustrated in Figure 1. The spectra exhibit two isosbestic

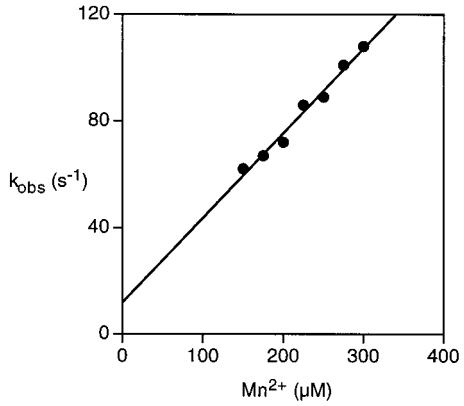

FIGURE 2: Concentration dependence of the observed rate constant for binding of $Mn(H_2O)_6^{2+}$ to FosA followed by the change in absorbance at 297 nm. The solid line is a linear regression fit of the data to the equation $k_{obsd} = k_{on}(app)[Mn^{2+}] + k_{off}(app)$. Values for apparent rate constants $k_{on}(app)$ and $k_{off}(app)$ are given in Table 1.

points at 267 and 287 nm. The time-dependent changes in the absorption spectra are best described by a simple single-step binding mechanism with no evidence for spectral intermediates. The rate of evolution of the UV difference spectrum follows a single exponential and exhibits a first-order dependence on the concentration of the metal ion as illustrated in Figure 2. The data are consistent with a simple single-exponential approach to equilibrium with an observed bimolecular rate constant $k_{on} = (3.0 \pm 0.2) \times 10^5$ M^{-1} s^{-1} and an apparent unimolecular $k_{off} = 12 \pm 5$ s^{-1}. However, the calculated dissociation constant $K_d^{Mn^{2+}} = k_{off}/k_{on} = 40$ μM is considerably higher than the experimental value of <1 μM (*1*). The UV spectral changes appear to report on only part of the metal binding process.

In contrast, the temporal changes in the intrinsic protein fluorescence on metal binding are much more complex. When Mn^{2+} is mixed with the protein, five distinct exponential decays are observed over a time span of 2 ms to several minutes (Figure 3). The first decay is kinetically identical to that observed in the absorption spectra showing a first-order dependence on the concentration of $Mn(H_2O)_6^{2+}$ (data not shown) and has the single largest amplitude, comprising ~60% of the total fluorescence signal. The four subsequent exponential decays are independent of the metal ion concentration and are similar in amplitude, each comprising ~10% of the total signal (Table 1). Control experiments using either enzyme alone or the preformed $E{\cdot}Mn^{2+}$ complex indicated that the slow concentration-independent decreases in fluorescence are not due to photobleaching of the protein. The fact that the rate constants describing the four slower phases are independent of $[Mn^{2+}]$ suggests that they may represent slow isomerizations of the protein that occur either prior to or after coordination complex formation. The inclusion of K^+ does not alter the kinetics of metal binding.

Binding of Mn^{2+} Is Accompanied by Rapid Proton Release. The addition of $Mn(H_2O)_6^{2+}$ to an unbuffered solution of FosA (20 μM active sites, pH 8.0) resulted in a decrease in the pH of the solution. Titration of the solution back to pH 8.0 required the addition of 2 equiv of hydroxide ion per subunit. Thus, it appears that binding of Mn^{2+} results in the release of two protons from each active site.

The kinetics of proton release was examined at pH 8.0 using the pH indicator phenol red ($pK_a = 7.9$). Rapid mixing

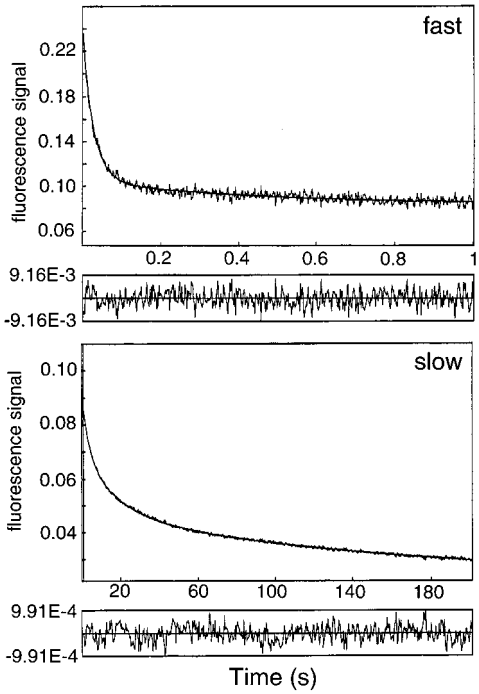

FIGURE 3: Changes in the intrinsic protein fluorescence following rapid mixing of 5 μM FosA with 100 μM $Mn(H_2O)_6^{2+}$ at pH 8.0. The top panel shows the changes observed from 2 ms to 1 s. The decay was fit to a double exponential with $k_{obsd1} = 36 \pm 1$ s^{-1} (amplitude $= 0.136 \pm 0.002$) and $k_{obsd2} = 2.5 \pm 0.3$ s^{-1} (amplitude $= 0.022 \pm 0.001$). The residual to this fit is shown under the top panel. The bottom panel shows the changes observed from 1 to 200 s. The slow decay was fit to a triple exponential with $k_{obsd3} = 0.27 \pm 0.01$ s^{-1} (amplitude $= 0.026 \pm 0.001$), $k_{obsd4} = 0.054 \pm 0.003$ s^{-1} (amplitude $= 0.023 \pm 0.001$), and $k_{obsd5} = 0.0055 \pm 0.0006$ s^{-1} (amplitude $= 0.026 \pm 0.001$). The bottom trace is the residual to this fit. Only k_{obsd1} is dependent on the concentration of $Mn(H_2O)_6^{2+}$.

Table 1: Observed Rate Constants for Changes in Protein Absorbance and Fluorescence on Binding $Mn(H_2O)_6^{2+}$

	method		
rate constant	absorption[a] (297 nm)	fluorescence (>320 nm)	relative fluorescence amplitude
$k_{on1}(app)$[b] (M^{-1} s^{-1})	$(3.2 \pm 0.2) \times 10^5$	$(3.0 \pm 0.1) \times 10^5$	0.59
$k_{off}(app)$[b] (s^{-1})	12 ± 5	13 ± 3	
k_{on2} (s^{-1})		2.5 ± 0.3	0.09
k_{on3} (s^{-1})		0.27 ± 0.01	0.11
k_{on4} (s^{-1})		0.054 ± 0.003	0.10
k_{on5} (s^{-1})		0.0055 ± 0.0006	0.11

[a] Absorption change follows a single exponential. An independent experiment at 245 nm gave $k_{on1}(app) = (2.9 \pm 0.1) \times 10^5$ M^{-1} s^{-1} and $k_{off}(app) = 6 \pm 2$ s^{-1}. [b] Obtained from the slope and intercept of the dependence of k_{obsd} on $[Mn^{2+}]$ as in Figure 2.

of equal volumes of sparged and unbuffered solutions of enzyme and $Mn(H_2O)_6^{2+}$ containing phenol red produced a very rapid decrease ($k_{obsd} \geq 800$ s^{-1}) in absorbance at 558 nm as illustrated in Figure 4. Although the decrease in A_{558} continues for ~5 s, the majority (>80%) of the reaction occurs with a relaxation time that is about the same as the mixing time of the instrument (≤2 ms). The rate of the rapid decrease in A_{558} appears to be independent of the concentration of the metal. That a large portion of the proton release occurs more rapidly than the changes observed in absorption or fluorescence suggests there is a very fast step prior to multidentate coordination of the metal. A small fraction

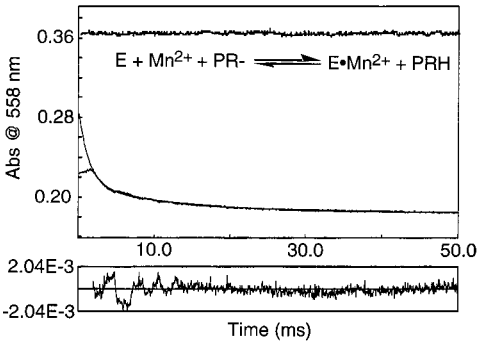

FIGURE 4: Fast change in absorbance at 558 nm upon rapid mixing of 10 μM FosA with 300 μM $Mn(H_2O)_6^{2+}$ at pH 8.0 and 25 °C in the presence of the pH indicator phenol red (PR). The top trace shows the baseline absorbance of phenol red and enzyme in the absence of $Mn(H_2O)_6^{2+}$. The decrease in A_{558} beyond the dead time of the instrument on mixing enzyme and metal was fit to a double exponential with $k_{obsd1} = 760 \pm 20$ s^{-1} (amplitude = 0.078) and $k_{obsd2} = 85 \pm 1$ s^{-1} (amplitude = 0.029). Note that the amplitudes of the two phases account for only ~60% of the total change in A_{558} of 0.18.

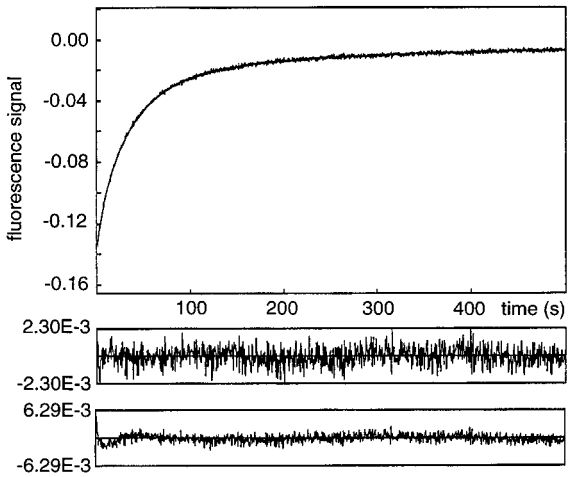

FIGURE 5: Determination of the rate of release of Mn^{2+} from FosA by trapping with EDTA. A solution of FosA and Mn^{2+} in 100 mM HEPES (pH 8.0) was rapidly mixed with an equal volume of EDTA in the same buffer. The final concentrations were 10 μM FosA, 25 μM Mn^{2+}, and 25 mM EDTA. The fluorescence recovery was best fit to a triple exponential with the rate constants reported in Table 2. The middle trace is the residual for the triple-exponential fit. The systematic error in the residual to a double-exponential fit of the same data is apparent in the lower trace, particularly in the first 50 s.

(~10%) of the change in A_{558} occurs with relaxation times of ≥300 ms.

Dissociation of Mn^{2+} Is Slow. The dissociation rate of the metal from the E·Mn^{2+} complex was determined by rapidly mixing the complex with a high concentration (25 mM) of EDTA. Dissociation of the metal was then followed by either the decrease in absorbance at 297 nm (data not shown) or the increase in intrinsic protein fluorescence (Figure 5) on formation of the free enzyme. The observed dissociation kinetics are independent of the concentration of EDTA (15−50 mM), indicating that the trapping reaction is not rate-limiting. Both spectral probes reveal a slow release of metal ion that occurs in three phases. The rate constants and amplitudes derived from the two techniques are similar (Table 2). The differences in rate constants and amplitudes obtained in the absorption and fluorescence experiments are primarily due to the lower precision of the absorption data

Table 2: Dissociation of Mn^{2+} from the E·Mn^{2+} Complex by EDTA Trapping

	absorption (297 nm)		fluorescence (>320 nm)	
rate process	k_{obsd} (s^{-1})	relative amplitude	k_{obsd} (s^{-1})	relative amplitude
k_{off1}	0.32 ± 0.06	0.12 ± 0.01	0.17 ± 0.01	0.14 ± 0.01
k_{off2}	0.032 ± 0.002	0.78 ± 0.06	0.029 ± 0.001	0.67 ± 0.01
k_{off3}	0.0081 ± 0.0056	0.10 ± 0.06	0.0057 ± 0.0003	0.19 ± 0.01

Scheme 1

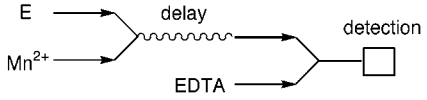

caused by a lower signal-to-noise ratio. Both sets of data suggest the formation of at least three tight protein−metal complexes after formation of an intermediate coordination complex. Assuming the extinction coefficients or quantum yields of the complexes are similar, the amplitudes of the spectral changes suggest that the complex with the dissociation rate of ~0.03 s^{-1} predominates at equilibrium.

Slowly Dissociating Species Are Formed Rapidly. If the tight metal complexes observed in the dissociation experiments are formed from an intermediate coordination complex, their rates of formation would be expected to be relatively fast. Alternatively, the observation of slow phases in the binding of the metal (above) could be interpreted as reflecting slow isomerizations of the intermediate complex to form tight binding species. If the tight metal complexes are formed slowly, then it should be possible to observe their formation as a function of time by trapping with EDTA.

To examine this question in more detail, a sequential mixing experiment, diagramed in Scheme 1, was designed to detect the formation of the tight complexes. Thus, the extent of tight complex formation as a function of time was determined by rapidly combining enzyme and metal and waiting a variable incubation (or delay) period before reversing the formation by rapid addition of EDTA; the release of metal is detected by the recovery of intrinsic fluorescence in the stopped flow. Fluorescence recovery data were collected for delay times between 0.02 and 100 s. At all of the measured delay times, the fluorescence recovery was best fit to a triple exponential with rate constants of 0.2, 0.03, and 0.006 s^{-1}. The relative amplitudes of the three phases were 0.15, 0.60, and 0.25, respectively, values very close to those reported in Table 2.

The overall amplitude of the fluorescence recovery increased between 0.02 and 0.5 s with a rise time of ~50 ms measured for species with a dissociation rate constant of 0.03 s^{-1} as illustrated in Figure 6. The rise time corresponds to a rate of tight complex formation of 14 s^{-1}, which is very close to the calculated rate of formation of the intermediate coordination complex [$(3 \times 10^5$ M^{-1} s$^{-1})(4 \times 10^{-5}$ M) = 12 s^{-1}]. Thus, the rate of formation of the tight complex is fast and appears to be limited by the rate of formation of the intermediate coordination complex. The signal amplitudes of the two other tight complexes are too small to get an accurate measure of their rise times. However, it is clear that all three species are detectable in the same relative concentrations almost instantaneously (≤20 ms). Small increases (~20%) in the signal amplitude associated with

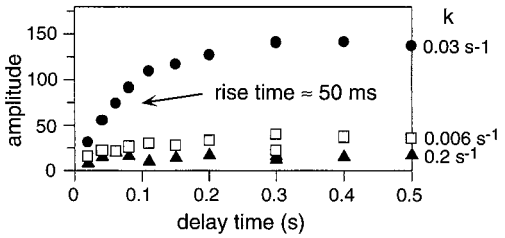

FIGURE 6: Sequential mixing of FosA, $Mn(H_2O)_6^{2+}$, and EDTA at pH 8.0 and 25 °C. FosA (4 μM) and $Mn(H_2O)_6^{2+}$ (40 μM) were incubated at various delay times in the aging loop and then rapidly mixed with EDTA. The recovery of the intrinsic protein fluorescence signal was fit to a triple exponential with rate constants of 0.2, 0.03, and 0.006 s^{-1}. The amplitudes of each kinetic phase are plotted as a function of the delay time.

all three species are seen at delay times between 0.5 and 100 s. This increase may be due to a fraction of the intermediate complex that forms or isomerizes slowly.

Effect of Fosfomycin on the Dissociation of Mn^{2+}. It has been proposed that the chemical mechanism of FosA involves a direct interaction of fosfomycin with the metal center (*1*). Not surprisingly, the presence of fosfomycin has little effect on the rate of association of $Mn(H_2O)_6^{2+}$ with the enzyme. The k_{on}(obsd) = (3.5 ± 0.1) × 10^5 M^{-1} s^{-1} in the presence of 0.4 mM fosfomycin is essentially the same as that observed in its absence (Table 1). However, the substrate does have a significant, concentration-dependent effect on certain aspects of the dissociation kinetics. The intercept term in the concentration-dependent association kinetics (Figure 2; Table 1) decreases by a relatively modest factor of ~4 to 3.2 ± 1.5 s^{-1}, suggesting a decrease in the off-rate of the metal.

A more dramatic effect is seen in the metal dissociation kinetics as determined in the EDTA trapping experiments. The rate constants, k_{off1} and k_{off3}, for the first and third exponential phases of the dissociation show modest, 3−6-fold, decreases on addition of fosfomycin. In contrast, there is a very significant decrease in k_{off2} describing the second dissociation event. This rate constant decreases by a factor of at least 25-fold upon titration of the $E{\cdot}Mn^{2+}$ complex with increasing concentrations of fosfomycin as illustrated in Figure 7. At high concentrations of fosfomycin (>1 mM) the metal dissociation kinetics become biphasic as the rate constant k_{off2} approaches that of k_{off3}. The concentration dependence of k_{off2} can be used to calculate an apparent K_d for fosfomycin of 15 ± 4 μM. This value is in reasonable agreement with the K_m for fosfomycin, which varies from 10 to 60 μM over the pH range of 7.5−8.5 (*17*).

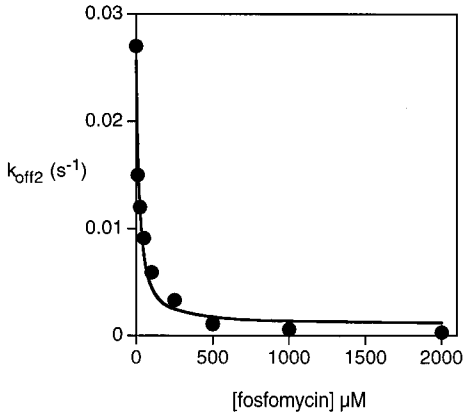

FIGURE 7: Dependence of the rate constant k_{off2} on the concentration of fosfomycin. A solution of FosA and $Mn(H_2O)_6^{2+}$ in 100 mM HEPES (pH 8.0) containing various concentrations of fosfomycin was rapidly mixed with an equal volume of EDTA at pH 8.0. The final concentrations were 10 μM FosA, 25 μM $Mn(H_2O)_6^{2+}$, 0−2 mM fosfomycin, and 25 mM EDTA. The rate constant k_{off2} was obtained by fitting the increase in fluorescence (≥320 nm) to a triple exponential (e.g., Figure 5). Where fosfomycin was ≥1 mM, the kinetic data were best fit to a double exponential because k_{off2} ≈ k_{off3}. The solid line is a nonlinear regression fit of the data to the equation $k_{off2} = (k_u([E{\cdot}Mn^{2+}]_t - [E{\cdot}Mn^{2+}{\cdot}S]) + k_b[E{\cdot}Mn^{2+}{\cdot}S])/[E{\cdot}Mn^{2+}]_t$, where k_u = 0.026 ± 0.002 s^{-1} is the rate constant for release with no fosfomycin bound and k_b = 0.001 ± 0.0009 s^{-1} is the rate constant with fosfomycin (S) bound. The concentration of the substrate-bound species $[E{\cdot}Mn^{2+}{\cdot}S]$ was obtained from the quadratic expression $[E{\cdot}Mn^{2+}{\cdot}S] = b - \sqrt{b^2-[4([E{\cdot}Mn^{2+}]_t)([S]_t)]}/2$, where $b = K_d + [S]_t + E{\cdot}Mn^{2+}]_t$ and K_d = 15 ± 4 μM is the dissociation constant for fosfomycin.

Scheme 2

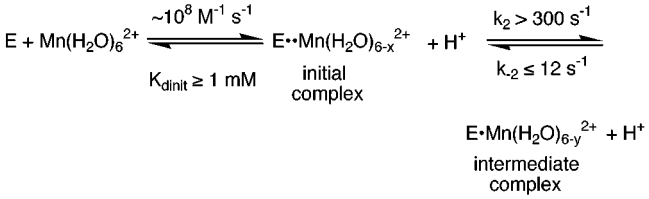

Scheme 3

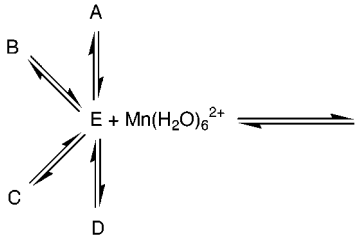

DISCUSSION

Formation of the Intermediate Complex. The apoFosA protein (pI ≈ 4.5) has a substantial negative charge at neutral pH. The initial events in the binding of $Mn(H_2O)_6^{2+}$ to FosA are likely facilitated by electrostatic attraction between the positively charged metal ion and the negative charge of the protein. Nevertheless, the binding of divalent metal results in the release of two protons at equilibrium, perhaps reflecting the tendency to preserve electroneutrality of the metal-binding site buried within the protein (*18*). The release of protons from FosA on mixing with $Mn(H_2O)_6^{2+}$ is rapid and occurs before any changes in the UV spectral characteristics of the protein are observed. This suggests that a substantial fraction of the proton release occurs upon formation of an initial complex prior to complete ligand exchange and formation of the spectroscopically detectable intermediate coordination complex as illustrated in Scheme 2. The extent to which formation of the initial complex (and proton release) involves inner sphere interactions between the protein and metal is not clear. A portion of the proton release, perhaps as much as 50%, occurs on the time scale of formation of the intermediate coordination complex as indicated in Scheme 2. Inasmuch as the rate of water exchange from $Mn(H_2O)_6^{2+}$ of 10^7 s^{-1} (*18*) is much faster than the observed proton release rates, it is likely proton release or associated conformational changes limit the rate of formation of the initial complex.

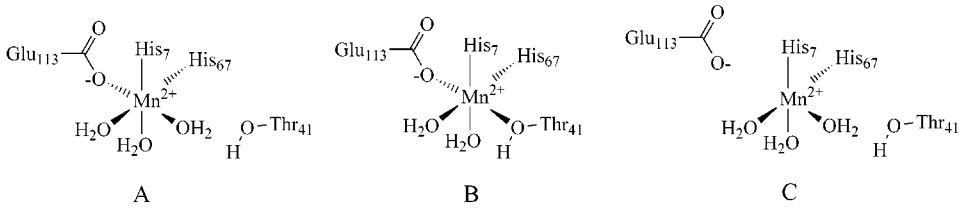

FIGURE 8: Possible alternate coordination geometries for the FosA·Mn^{2+} complex.

Scheme 4

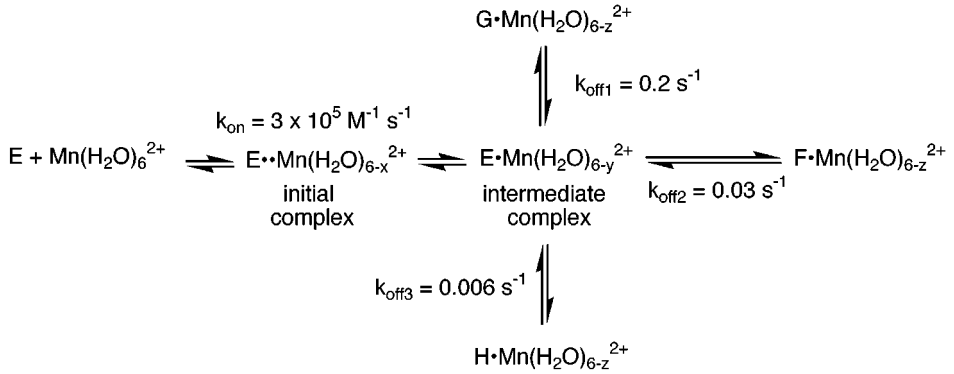

The observed bimolecular rate constant for formation of the intermediate complex $k_{obsd} = 3 \times 10^5\ M^{-1}\ s^{-1}$ in Scheme 2 is given by the expression $k_{obsd} = k_{-2} + k_2[M]/([M] + K_{dinit})$, where K_{dinit} is the dissociation constant for the initial complex. The initial complex, which is signaled only by the loss of protons, is likely to be quite loose because it is preparatory to formation of the intermediate complex. If K_{dinit} for the formation of the initial complex is much larger than [M], then $k_{obsd} = k_{-2} + (k_2/K_{dinit})[M]$. This condition is satisfied if $K_{dinit} \geq 1$ mM and $k_2 > 300\ s^{-1}$. The upper limit on k_{-2} of 12 s^{-1} is derived from the intercept of plots of k_{obsd} versus [Mn^{2+}] as in Figure 2. The actual value of k_{-2} may be smaller depending on the contributions of subsequent kinetic events to the magnitude of the intercept.

Slow Steps in the Acquisition of Mn^{2+}. The changes in the fluorescence of the protein on binding $Mn(H_2O)_6^{2+}$ suggest that there are several slow, concentration-independent events involved in the acquisition of metal. It is not possible to quantify the contribution of these events and the species they represent to the overall kinetic process because the fluorescence quantum yields for the species are not known. One possible explanation of the slow events is that the apoenzyme consists of an ensemble of as many as five conformational isomers, only one of which can easily form the intermediate coordination complex. One possibility for this type of behavior is represented in Scheme 3, where species A−D are in slow equilibrium with the metal receptive species, E. If the fluorescence spectral properties of species A−D are similar, then the amplitudes of the four slow kinetic phases suggest that the four species are nearly equally populated. However, the total concentration of these species must be quite low (<10%) with respect to [E]. Otherwise, their contribution to the formation of the coordination complex would be detected as a slow concentration-independent change in the absorption spectra.

Obviously, other schemes with linked equilibria are possible and the nature of the species involved in the slow processes is unknown. They could be partially unfolded protein or rare conformers that primarily occur in the absence of metal. Gel filtration experiments indicate the enzyme is a dimer in the absence of metal ion. Therefore, it is unlikely that species A−D represent different oligomeric states of the protein.

Tight Binding of Mn^{2+}. The EDTA trapping experiments suggest that there are at least three species with relatively small apparent rate constants for the dissociation of metal. One possibility is shown in Scheme 4. The apparent rate constants for metal release reflect slow isomerizations of the three species to the intermediate complex from which metal is rapidly released. It appears that the most highly populated of these has a dissociation rate constant of 0.03 s^{-1} or a half-life in excess of 20 s. The sequential mixing experiments indicate that all three species form as rapidly as does the initial coordination complex. It is therefore unlikely that the slow fluorescence changes observed upon Mn^{2+} binding represent spectral changes associated with formation of the slowly dissociating complexes. It is not clear if any or all of the slowly dissociating complexes have spectral properties that are significantly different from those of the initial coordination complex. If the spectral properties are the same, then the observed spectral change on metal binding and release is due entirely to the formation of the intermediate complex from free enzyme and metal. In this instance amplitudes of each slow phase in the EDTA trapping experiments would directly reflect the abundance of each of the three species at equilibrium (Scheme 4).

The structural differences among the kinetically observed F·Mn^{2+}, G·Mn^{2+}, and H·Mn^{2+} complexes are obviously not known at this juncture. The predominant complex is likely to be that shown in Figure 8A. The others may reflect alternate coordination isomers for the metal complex involving loss of a ligand (H7, H67, or E113) or conscription of an additional protein ligand. The FosA enzyme is a member of an evolutionarily divergent family of proteins that includes other metalloenzymes such as the extradiol dioxygenases, glyoxalase I and methylmalonyl CoA epimerase (*1*, *4*, *8*, *9*). Glyoxalase I and methylmalonyl CoA epimerase are known to supply four ligands to the octahedral coordination sphere

of their respective metal ions with the other two sites occupied by water (*19*−*22*). In contrast, the dioxygenases, like FosA, supply only three ligands to the metal, usually Fe^{2+}, and have three open or solvent-occupied coordination sites in the absence of the substrates (*23*, *24*). Comparison of the crystal structures of these enzymes suggests that one ligand in glyoxalase I (E56) is replaced with alanine in the dioxygenase (*8*). Although the structure of FosA is not known, multiple sequence alignments suggest that the corresponding residue in FosA is T41 (*4*, *9*). Thus, one alternate, rarely populated coordination isomer might involve the hydroxyl group of T41 replacing one of the three water molecules (Figure 8B).

Alternatively, these complexes may reflect, in part, a natural flexibility in the coordination environment of the metal that is necessary for efficient catalysis. Recent spectroscopic evidence[2] suggests that the coordination environment about the metal undergoes a dramatic change in which the E113 ligand moves out of the inner coordination sphere upon binding the substrate fosfomycin (*1*, *4*). The net effect of this change is to increase the electrophilicity of the metal and hence its effectiveness in catalysis. It is possible that even in the absence of fosfomycin a small fraction of the coordination complex is essentially a bidentate protein−metal complex with E113 out of the inner coordination sphere (Figure 8C).

Coordination of Fosfomycin at the Metal Center. A number of lines of evidence suggest that fosfomycin forms an inner sphere coordination complex with the mononuclear metal center. Solvent molecules appear to occupy three of the six coordination sites of the metal so that coordination sites are available. In addition, the rather remarkable change in the EPR spectrum of enzyme-bound Mn^{2+} on addition of fosfomycin indicates a substantial distortion in the symmetry of the coordination sphere of the metal on substrate binding (*1*).[2] The fact that fosfomycin reduces the rate of dissociation of Mn^{2+} from the most abundant enzyme−Mn^{2+} complex in a concentration-dependent manner is also consistent with the idea of an inner sphere complex between the substrate and enzyme-bound metal being formed. The apparent dissociation constant of 15 ± 4 μM for fosfomycin from titration of k_{off2} (Figure 7) is in reasonable, although not perfect, agreement with the K_d of 17 ± 2 μM obtained from titration of the water proton relaxation rate (*1*) or the K_m of the substrate (48 ± 3 μM) at pH 8 (*17*). The presence of fosfomycin also modestly slows the release Mn^{2+} from the other two species detected in the release experiments, a result that suggests the substrate interacts to some degree with all metal binding species.

Conclusions. The binding of $Mn(H_2O)_6^{2+}$ to apoFosA occurs in a multistep process involving the reversible formation of an initial complex that rapidly collapses to an intermediate coordination complex. These processes involve the release of approximately two protons. The intermediate complex rapidly isomerizes to a set of tight metal complexes from which the release of metal is quite slow. The addition of fosfomycin has no discernible effect on the association rate of the metal with the protein. However, the rate of release of metal from the protein in the presence of fosfomycin is diminished by a factor of 25 for the predominant complex, suggesting that the substrate alters and probably participates in the coordination of the metal.

[2] The binding of fosfomycin to the FosA·Mn^{2+} complex results in a change in the axial zero-field splitting from $|D| = 0.06$ cm^{-1} in the substrate-free enzyme to $|D| = 0.28$ cm^{-1} in the substrate-bound state. Ligand field analysis suggests that this change reflects a significant alteration in the Mn^{2+} coordination environment perhaps involving a movement of E113 out of the inner sphere (Smoukov, S., Telser, J., Bernat, B. A., Rife, C. L., Armstrong, R. N., and Hoffman, B. M., submitted for publication).

REFERENCES

1. Bernat, B. A., Laughlin, L. T., and Armstrong, R. N. (1997) *Biochemistry 36*, 3050−3055.
2. Armstrong, R. N. (1998) *Curr. Opin. Chem. Biol. 2*, 618−623.
3. Laughlin, L. T., Bernat, B. A., and Armstrong, R. N. (1998) *Chem.-Biol. Interact. 111*, 41−50.
4. Bernat, B. A., Laughlin, L. T., and Armstrong, R. N. (1999) *Biochemistry 38*, 7462−7469.
5. Armstrong, R. N. (1997) *Chem. Res. Toxicol. 10*, 2−18.
6. Babbitt, P. C., and Gerlt, J. A. (1997) *J. Biol. Chem. 272*, 30591−30594.
7. Arca, P., Rico, M., Brana, A. F., Villar, C. J., Hardisson, C., and Suarez, J. E. (1988) *Antimicrob. Agents Chemother. 32*, 1552−1556.
8. Bergdoll, M., Eltis, L. D., Cameron, A. D., Dumas, P., and Bolin, J. T. (1998) *Protein Sci. 7*, 1661−1670.
9. Armstrong, R. N. (2000) *Biochemistry 39*, 13625−13632.
10. Pocker, Y., and Fong, C. T. O. (1983) *Biochemistry 22*, 813−818.
11. Buchsbaum, J. C., and Berg, J. M. (2000) *Inorg. Chim. Acta 297*, 217−219.
12. Eigen, M., and Hammes, G. G. (1963) *Adv. Enzymol. 25*, 1−38.
13. Kiefer, L. L., Paterno, S. A., and Fierke, C. A. (1995) *J. Am. Chem. Soc. 117*, 6831−6837.
14. Drake, S. K., and Falke, J. J. (1996) *Biochemistry 35*, 1753−1760.
15. Shim, H., and Raushel, F. M. (2000) *Biochemistry 39*, 7357−7364.
16. Hunt, J. A., and Fierke, C. A. (1997) *J. Biol. Chem. 272*, 20364−20372.
17. Bernat, B. A. (1999) Mechanistic Studies of the Fosfomycin Resistance Protein FosA: A Novel Manganese Metalloglutathione Transferase, Ph.D. Dissertation, Vanderbilt University, Nashville, TN.
18. Lippard, S. J., and Berg, J. M. (1994) *Principles of Bioinorganic Chemistry*, pp 218−221, University Science Books, Mill Valley, CA.
19. Cameron, A. D., Olin, B., Ridderstom, M., Mannervik, B., and Jones, T. A. (1997) *EMBO J. 16*, 3386-3395.
20. Cameron, A. D., Ridderstrom, M., Kavarana, M. J., Creighton, D. J., and Mannervik, B. (1999) *Biochemistry 38*, 13480−13490.
21. He, M. M., Clugston, S. L., Honek, J. F., and Matthews, B. W. (2000) *Biochemistry 39*, 8719−8727.
22. McCarthy, A. A., Baker, H. M., Shewry, S. C., Patchett, M. L., and Baker, E. N. (2001) *Structure 9*, 637−646.
23. Han, S., Eltis, L. D., Tmmis, K. N., Muchmore, S. W., and Bolin, J. T. (1995) *Science 270*, 976−980.
24. Shu, L., Chiou, Y.-M., Orville, A. M., Miller, M. A., Lipscomb, J. D., and Que, L. (1995) *Biochemistry 34*, 6649−6659.

BI0114832